Simultaneous quantification of aquatic ecosystem metabolism and reaeration using a Bayesian statistical model of oxygen dynamics

Gordon W. Holtgrieve,[a,b,*] Daniel E. Schindler,[a] Trevor A. Branch,[a] and Z. Teresa A'mar[a]

[a] School of Aquatic and Fishery Sciences, University of Washington, Seattle, Washington
[b] Department of Biology, University of Washington, Seattle, Washington

Abstract

We present a Bayesian statistical model of diel oxygen dynamics in aquatic ecosystems to simultaneously estimate gross primary production, ecosystem respiration, and oxygen exchange with the atmosphere (and their uncertainties) on the basis of changes in dissolved oxygen concentration, water temperature, irradiance, and, if desired, the ^{18}O to ^{16}O ratio ($\delta^{18}O–O_2$). We test this model using simulated data with realistic measurement errors to demonstrate that it accurately estimates the model parameters and that parameter uncertainties correctly scale with error in the observations and number of data points. Application of the model to field data from two productive stream ecosystems with substantial daily dissolved oxygen variation quantified the underlying physical and biological factors that control oxygen dynamics in these ecosystems and provided empirical support for a light saturation model of the photosynthesis–irradiance relationships at the ecosystem scale. Although inclusion of $\delta^{18}O–O_2$ provides a second oxygen budget, analysis of field data shows that metabolic and reaeration parameters can be accurately estimated by modeling the transient dynamics of dissolved oxygen concentration alone in relation to daily changes in water temperature and light regime. This model is particularly suited to low–gas exchange, high-productivity systems, which have thus far proved challenging to measure ecosystem metabolism accurately. The modeling framework is applicable to single-station, open-system experimental designs and provides a rigorous and generalizable framework for estimating ecosystem metabolism in aquatic ecosystems.

Quantifying the assimilation and transformation of energy is fundamental to our understanding of how ecosystems function (Lindeman 1942). The process of acquiring external energy through carbon fixation, and subsequent carbon oxidation via respiration, is a basal feature of all ecosystems. In fact, the most basic descriptors of aquatic ecosystems (eutrophic or oligotrophic, heterotrophic or autotrophic) refer directly to relative ecosystem productivity. The trophic state of an ecosystem affects nearly all ecological interactions, including species relationships, patterns of biodiversity, biogeochemical cycling, and system stability. Quantifying rates of primary production and respiration, and the relative dominance between the two, is therefore critical to our understanding of energy flows and nutrient cycling, allochthony and autochthony, trophic state, and food web dynamics in aquatic ecosystems.

Odum (1956) first addressed questions of how ecosystem metabolism varies across seasonal cycles, among ecosystem types, and in response to anthropogenic environmental change. However, in spite of this long history, essentially the same sets of questions remain largely unresolved and are an active area of ongoing research (Mulholland et al. 2005; Roberts et al. 2007). No single method has emerged as the standard for measuring ecosystem metabolism, and comparisons among methods often produce inconsistent results (Juranek and Quay 2005; Yacobi et al. 2007). In vitro methods for quantifying rates of primary production and respiration include light- and dark-bottle incubations and uptake of radiocarbon (C-14) by biota (the latter does not include respiration; Howarth and Michaels 2000).

Open-system diel oxygen mass balance methods are commonly applied to productive streams and lakes in which metabolic rates are high relative to the size of dissolved oxygen pools and air–water gas transfer can be estimated with tracer experiments or standard empirical relationships (Odum 1956; Marzolf et al. 1994). More recently, dual (^{16}O, ^{18}O) and triple (^{16}O, ^{17}O, ^{18}O) stable isotope measurements of dissolved oxygen have been used as natural tracers of metabolic processes in ocean and large-river ecosystems that approximate steady-state conditions (Emerson et al. 1995; Quay et al. 1995; Luz and Barkan 2000). The requirement for an independent determination of the gas transfer velocity to estimate air–water exchange with all open-system methods also creates substantial additional uncertainty, and, possibly, bias, which are usually not incorporated into metabolism estimates.

Put simply, estimates of ecosystem metabolic properties rely on a variety of techniques, many of which are cumbersome and all of which introduce substantial errors that are difficult to quantify directly.

Sources of error and incorporating prior information— The above approaches generally fail to consider uncertainty, both in how ecological models are parameterized and in interpreting results. Without full consideration of uncertainty, complete examination of mechanisms controlling ecosystem metabolism, as well as implications of widespread environmental change (e.g., climate change, eutrophication), will remain elusive. Uncertainty in the analysis of ecological systems typically can arise from three sources: observation uncertainty, process uncertainty, and model uncertainty (Francis and Shotton 1997; Hilborn and Mangel 1997). Observation uncertainty is associated with

---

Table 1. BaMM parameters.

Geographic and physical parameters	Measured diel data	Model-estimated parameters*
Latitude (decimal degrees)†	Local time (h)	α_{P-I} (mg O_2 s μE^{-1} h^{-1})
Longitude (decimal degrees)†	Water T (°C)	P_{max} (mg O_2 m^{-2} h^{-1})‡
Altitude (m)	PAR irradiance (μE s^{-1} m^{-2})	R_{20} (mg O_2 m^{-2} h^{-1})
Aspect†	O_2 concentration (mg L^{-1})	k_{20} (m h^{-1})
Slope†	$\delta^{18}O$–O_2 (‰ vs. SMOW)§	α_R||
Time zone (hours relative to GMT)†		$\delta^{18}O$–H_2O (‰ vs. SMOW)||
Daylight savings time (h)†		Initial O_2 concentration (mg L^{-1})
Transmissivity†		Initial $\delta^{18}O$–O_2 (‰ vs. SMOW)||
Area (m^2)		σ O_2 concentration
Depth (m)		σ $\delta^{18}O$–O_2||
Salinity (g kg^{-1})		

SMOW, standard mean ocean water.
* Model parameters can be fixed constants or incorporate prior information as uniform or normal distributions (*see* text for parameter abbreviations).
† Required only if using modeled irradiance.
‡ Estimated in addition to α_{P-I} under light-saturation assumption.
|| Estimated only if including $\delta^{18}O$–O_2 data.
§ Optional.

inconsistencies in measurement technique (precision) and measurement bias (accuracy). All measurements contain some level of error that, when quantified, can (and should) be readily incorporated into ecological models. Process uncertainty arises from inherent stochasticity or natural variability of system components that are extrinsic to the processes being modeled. Finally, model uncertainty is the inability of a specified model to fully describe the biological or physical process in the ecosystem.

In addition to quantitative analysis of measured ecological data, incorporating prior information in a statistically relevant manner is important to the interpretation of data, especially when measurements have a high degree of uncertainty (Hilborn and Mangel 1997). For example, oxygen mass balance methods for calculating ecosystem metabolism in open systems depend critically on the rate of reaeration (gas exchange across the air–water interface) and are highly sensitive to changes in this parameter (Tobias et al. 2009). There is no one best method for estimating reaeration across ecosystem types (examples include empirical models based on wind speed for large open water systems or deliberate tracer injections for smaller lotic systems) and the relative precision of these estimates varies by methods, system, and experimenter. In many systems, such as medium to large rivers and estuaries, existing methods are inadequate and have limited rigorous ecosystem metabolism research in these systems. Disregard for the known or possibly unknown error structure when applying reaeration (or other critical parameters) will certainly overestimate confidence in the results. Similarly, incorporating error, without regard to whether extreme values are even possible given the data, runs the risk of making the results so vague as to be useless. These decisions are often left as 'judgment calls.' However, modern Bayesian methods allow for incorporation of this sort of prior information in a statistically robust manner (Hilborn and Mangel 1997).

Application of dynamic models and Bayesian analysis to measurements of ecosystem metabolism—In this paper, we describe an oxygen mass balance model organized within a Bayesian statistical framework (herein referred to as "BaMM" for Bayesian metabolic model) to simultaneously estimate ecosystem metabolic and reaeration rates from field observations of diel dynamics in dissolved oxygen. This model reconstructs the diel cycle of dissolved oxygen concentration ($[O_2]$) and the ^{18}O to ^{16}O ratio of dissolved oxygen ($\delta^{18}O$–O_2) at a single station as a function of several physical and biological parameters (Table 1). When supplied with measured $[O_2]$, water temperature, irradiance, and, if available, $\delta^{18}O$–O_2 data, the model estimates probability distributions of key ecosystem parameters, including gross primary production, ecosystem respiration, reaeration, and photosynthesis–irradiance relationships based on model fits to the data. Prior information, including measurement errors, can be specified for many of the parameters and incorporated into overall estimates of oxygen dynamics.

Methods

The dissolved oxygen pool in an aquatic ecosystem is controlled by three simultaneous processes: (1) respiration (here defined as all oxygen-consuming reactions within an ecosystem), (2) production of oxygen by photosynthesis (autotrophic production), and (3) reaeration or gas exchange with the atmosphere (Fig. 1). In productive ecosystems, there are often strong diel cycles of dissolved oxygen. Oxygen concentrations build with increasing light intensity (irradiance) as photosynthesis releases O_2 into the water. Respiration is a function of temperature, resulting in a gradual drawdown in dissolved oxygen during periods with low light intensity. Differences between daytime increases and nighttime declines in dissolved oxygen can therefore provide information on rates of photosynthesis and respiration, assuming reaeration can be adequately determined. Because of the mass dependent fractionations of respiration and gas exchange, the additional measurement of $\delta^{18}O$–O_2 provides a second, independent oxygen budget to quantify rates of biological processes (Quay et al. 1995; Venkiteswaran et al. 2007).
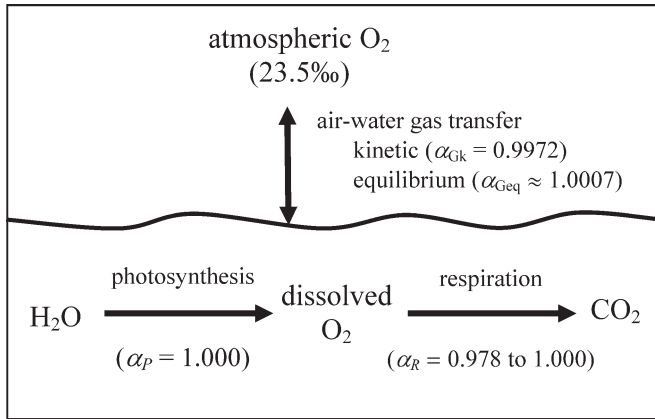
Fig. 1. Schematic diagram of oxygen pools and ecosystem metabolic processes included in the Bayesian Metabolic Model (BaMM). Arrows indicate fluxes among pools. Values in parentheses are $\delta^{18}O$ signatures of pools (vs. SMOW) or fractionations factors (α) of specific metabolic processes.

Given a set of model parameters describing photosynthesis, respiration, reaeration, and initial conditions, BaMM generates trajectories of dissolved oxygen concentration and $\delta^{18}O–O_2$ through time. These trajectories are then compared with observed diel data, which, with the use of Bayesian methods, allows for the selection of parameter values that do the best job of reconstructing the observed data.

To generate dissolved oxygen trajectories, BaMM relies on a series of interrelated equations that describe photosynthesis, respiration, and reaeration, and combines these processes to construct a mass balance of ^{16}O and ^{18}O of dissolved oxygen. BaMM also includes a submodel of photosynthetically active irradiance in case direct measurements are not available. BaMM was originally adapted from the PoRGy model presented in Venkiteswaran et al. (2007) and is ultimately based on the isotope mass balance equations presented in Quay et al. (1995). Oxygen pools are modeled as a system of differential equations and thus do not assume a steady-state condition—an assumption often violated in productive ecosystems (Parker et al. 2005; Tobias et al. 2007; Venkiteswaran et al. 2008). The ability of BaMM to track the transient (nonequilibrium) dynamics of aquatic oxygen in response to changing light intensity and temperature is what ultimately enables the simultaneous estimation of metabolic and reaeration parameters.

Dynamic dissolved oxygen and $\delta^{18}O–O_2$ model components—Photosynthesis: Photosynthesis can be modeled as having either a light-saturated or nonsaturated relationship. Equation 1 calculates photosynthesis (P) as a function of irradiance when light is saturating,

$$P(I) = P_{max}\tanh\left(\frac{\alpha_{P\text{-}I}I}{P_{max}}\right) \tag{1}$$

where I is the instantaneous irradiance ($\mu E\ s^{-1}\ m^{-2}$), P_{max} is production of oxygen at light saturation, and $\alpha_{P\text{-}I}$ is the slope of the photosynthesis–irradiance relationship at low light conditions (Jassby and Platt 1976). If the system is never light-saturated at the time of sampling, P is simply a linear function of irradiance (Eq. 2).

$$P(I) = \alpha_{P\text{-}I}I \tag{2}$$

Under a light-saturated assumption, both P_{max} and $\alpha_{P\text{-}I}$ are estimated as constants, whereas if light is not saturating, then only $\alpha_{P\text{-}I}$ needs to be estimated.

Irradiance submodel—Irradiance incident to the water surface can be calculated for a specified time frame and geographical position. The model is based on the surface full spectrum irradiance model (W m^{-2}) presented in Venkiteswaran et al. (2007) but has been adjusted to predict photosynthetically active radiation (PAR; 400–700 nm) in units of microEinsteins (μE, s^{-1} m^{-2}) to match the output of most commercial sensors (*see* Table 2 for conversion factors). Users can specify atmospheric transmissivity, but the model does not directly account for cloud cover or shading from local features such as mountains or trees. It is possible to rescale the irradiance model output to match measured PAR. Alternatively, and more desirably, directly measured PAR from a single station can be used in BaMM as long as data are available for all time points being modeled. PAR measurements should be representative of the full upstream reach contributing to O_2 dynamics at the sampling station.

Respiration—Respiration (R) is modeled as a temperature-dependent process as described by the van't Hoff–Arrhenius equation (Eq. 3; Venkiteswaran et al. 2007).

$$R(T) = R_{20}1.047^{(T-20)} \tag{3}$$

T (°C) is the observed water temperature. This model assumes all diel changes in R are determined by variation in water temperature (i.e., does not incorporate light-driven

Table 2. BaMM fixed constants.

Parameter	Value	Reference
α_P	1.000	Stevens et al. 1975; Guy et al. 1993; Helman et al. 2005
α_{Gk}	0.9972	Knox et al. 1992
α_{Geq}	1.0007	Benson et al. 1979; Benson and Krause 1984
$^{18/16}O$ of air	0.00205232	Kroopnick and Craig 1972
Full spectrum irradiance (W m^{-2}) to PAR (W m^{-2})	0.45	Gates 1966; Jellison and Melack 1993
PAR (W m^{-2}) to PAR (μE s^{-1} m^{-2})	4.57	McCree 1972

changes in autotrophic respiration) and includes all oxygen-consuming reactions, including heterotrophic respiration, chemical oxidation (i.e., nitrification), and photo-oxidation. Standardizing respiration to a constant temperature (R_{20} = respiration at $T = 20°C$) filters out daily or seasonal changes in water temperature and allows for more direct comparison of ecosystem change over time.

The fractionation factor on ^{18}O associated with respiration (α_R in Eq. 9) has been measured for open-water communities by bottle incubations with resulting values ranging from 0.978 to 0.982 (Kroopnick 1975; Quay et al. 1995; Quinones-Rivera et al. 2007). Systems with predominantly benthic communities (i.e., streams) have far fewer direct measurements of α_R. Incubation of stream sediment cores and slurries showed an average α_R of 0.987, suggesting possible substantial differences in the net community α_R among ecosystem types (Tobias et al. 2007). BaMM includes α_R as an estimated parameter, allowing for uncertainty in its value.

Gas exchange—The molecular diffusivity of O_2 across the air–water interface is described by the gas transfer velocity parameter (k, m h^{-1}). The magnitude of this parameter is determined by surface turbulence, water viscosity, and the solubility of O_2. Water viscosity and solubility are in turn a function of water temperature and salinity, as encapsulated by the Schmidt number (Sc). BaMM includes k at 20°C for freshwater (k_{20}) as an estimated parameter, which is then internally adjusted for observed salinity and water temperature at each time point using the Schmidt numbers and the following equations. The Schmidt number for O_2 in freshwater (FW) at a given water temperature (T, °C) is (Wanninkhof 1992):

$$\mathrm{Sc_{O_2,FW}}(T) = 1800.6 - 120.10T + 3.7818T^2 - 0.047608T^3 \quad (4)$$

The Schmidt number is then adjusted linearly for increasing salinity (S, g kg^{-1}),

$$\mathrm{Sc_{O_2}}(T, S) = \mathrm{Sc_{O_2,FW}}(1 + S \times m) \quad (5)$$

where the coefficient m is a linear function of water temperature calculated as (R. Wanninkhof pers. comm.):

$$m(T) = 3.286 \times 10^{-5}T + 2.474 \times 10^{-3} \quad (6)$$

The gas transfer velocity (k) at the observed water temperature and salinity is calculated with the Schmidt numbers and Eq. 7,

$$k(T, S) = k_{20}\left[\frac{\mathrm{Sc_{O_2}}(T, S)}{\mathrm{Sc_{O_2}}(20, 0)}\right]^{-0.5} \quad (7)$$

where, the exponent -0.5 is the accepted value for systems with waves at the air–water interface (Wanninkhof 1992). The denominator is the Schmidt number for O_2 in freshwater at 20°C and is equal to 530.46.

Mass balance equations—Dissolved oxygen concentration is a function of gas exchange with the atmosphere, oxygen-consuming reactions (respiration), and photosynthetic production of O_2 (Fig. 1). The equation describing the time rate of change in the dissolved oxygen pool is

$$\frac{d[O_2]}{dt} = [k([O_{2,sat}] - [O_2]) - R + P]/D \quad (8)$$

where $[O_2]$ is the dissolved oxygen concentration (mg m^{-3}), $[O_{2,sat}]$ is the dissolved oxygen concentration at atmospheric equilibrium, R is the instantaneous respiration rate, P is the instantaneous rate of photosynthesis (R and P are in units of mg O_2 m^{-2} h^{-1}), and D is the average mixed layer depth. The first term in Eq. 8 is the net effect of gas exchange, which is simply the gas transfer velocity (k) times the O_2 concentration gradient. $[O_{2,sat}]$ is calculated for a given water temperature and salinity as described in Weiss (1970).

The concentration of ^{18}O as dissolved oxygen ($[^{18}O-O_2]$, in mg m^{-3}) is controlled by the same processes as $[O_2]$ but must be adjusted for process-specific fractionation factors (α) and the isotopic ratios of the given pools (Fig. 1). The equation incorporating these processes is:

$$\frac{d[^{18}O-O_2]}{dt} = \left[k\alpha_{Gk}\left(O_{2,sat}\,{}^{18}_{16}O_{air}\alpha_{Geq} - O_2\,{}^{18}_{16}O_{DO}\right) - R\,{}^{18}_{16}O_{DO}\alpha_R + P\,{}^{18}_{16}O_{H_2O}\alpha_P\right]\Big/D \quad (9)$$

Where ${}^{18}_{16}O_{DO}$ is the isotopic ratio of dissolved oxygen, ${}^{18}_{16}O_{air}$ is the isotopic ratio of atmospheric O_2, and ${}^{18}_{16}O_{H_2O}$ is the isotopic ratio of oxygen in the water molecule. The fractionation factors α_R, α_P, α_{Gk}, and α_{Geq} are for respiration, photosynthesis, and the kinetic and equilibrium effects of gas exchange, respectively (*see* Table 2 for specific values).

Bayesian analysis—Bayesian analysis is a means to evaluate competing descriptions of nature with the use of all available information (Hilborn and Mangel 1997) and is based on Bayes theorem:

$$\mathrm{Pr}(M_i|D) = \frac{L(D|M_i)p(M_i)}{\sum\limits_{i=1}^{n} L(D|M_i)p(M_i)} \quad (10)$$

Bayes theorem states that the posterior probability of a particular model describing nature (M_i), given a set of data (D), is equal to the likelihood of observing the data given that model, times the prior probability of model M_i—that is, $p(M_i)$. The integral in the denominator of Eq. 10 acts to normalize the posterior probability of the model $\mathrm{Pr}(M_i|D)$ so that the probability of any particular model is always between 0 and 1. In BaMM, different sets of parameter values that produce diel $[O_2]$ and $\delta^{18}O–O_2$ curves can be thought of as competing models that are compared under Bayes theorem using the posterior probability. The combined likelihood of the data is the product of the individual likelihoods for observed $[O_2]$ data and, if available, $\delta^{18}O–O_2$ and is calculated as

$$L(D|M_i) = \prod_{j=1}^{n} \frac{1}{\sigma_{O_2,i}\sqrt{2\pi}} \exp\left[-\frac{(X_j - \mu_j)^2}{2(\sigma_{O_2,i})^2} \right]$$

$$\times \prod_{l=1}^{m} \frac{1}{\sigma_{^{18}O_2,i}\sqrt{2\pi}} \exp\left[-\frac{(X_l - \mu_l)^2}{2(\sigma_{^{18}O_2,i})^2} \right] \quad (11)$$

where $j = 1, \ldots, n$ are the individual $[O_2]$ data points and $l = 1, \ldots, m$ are the $\delta^{18}O–O_2$ data points. X_j and X_l are the observed values for $[O_2]$ and $\delta^{18}O–O_2$, respectively, whereas μ_j and μ_l are the predicted values. σ_{O_2} and $\sigma_{^{18}O_2}$ are the standard errors around $[O_2]$ and $\delta^{18}O–O_2$ values.

Prior information about k_{20}, α_R, $\delta^{18}O–H_2O$, σ_{O_2}, and $\sigma_{^{18}O_2}$ can be incorporated into BaMM by specifying a mean and standard deviation following a normal distribution. Alternatively, priors are specified as uniform distributions (a range of equally probable values) or, if it is assumed that parameters are known without any uncertainty, these parameters may be fixed as constants. It is assumed that no prior information exists to describe the system photosynthesis–irradiance relationship (P_{max} and α_{P-I}) or R_{20}.

BaMM identifies parameter combinations resulting in high posterior probabilities of the model given the data ($M_i|D$). This is achieved though implementation of a Markov Chain Monte Carlo (MCMC) algorithm, which generates a random walk through the parameter space, sampling values of each parameter in proportion to the total likelihood. For computational efficiency, the objective function in BaMM is the negative log of the total likelihood in Eq. 11; smaller values are therefore deemed to have higher evidential support.

Model parameter and ecosystem metabolism estimates— For every parameter combination saved in the MCMC chain, BaMM outputs the value of each parameter in that MCMC draw, the predicted $[O_2]$ and $\delta^{18}O–O_2$ for each time step in the model, and the instantaneous rates of ecosystem metabolism (P and R) plus reaeration for each time step in the model. Instantaneous P is calculated with the specified production function (Eq. 3 or 4) and irradiance. Instantaneous R is calculated with Eq. 5 and measured water temperature. Therefore, it is possible to plot best fit photosynthesis and irradiance relationships (P-I curves), as well as diel changes in P, R, and reaeration. BaMM also calculates integrated daily estimates of ecosystem metabolism with the use of a 24-h moving window average of the estimated instantaneous rates. We refer to these integrated daily values as gross primary production (GPP), ecosystem respiration (ER), and total mass flux of O_2 via gas exchange (G) to distinguish them from instantaneous rates for any one point in the diel period.

Model validation—BaMM estimates the values of up to 10 model parameters (Table 1). We conducted a set of stochastic simulations to ensure that model estimates of parameters can be realistically obtained from the kind of data that are typically collected in the field and to examine the effects of increasing observation error (precision and

accuracy), data resolution, and magnitude of diel changes in dissolved oxygen on the ability of BaMM to estimate model parameters (Hilborn and Walters 1992). The model itself was used to generate sets of diel oxygen pseudodata from prespecified parameter values, which were then thinned to an appropriate field collection resolution and random error applied. These pseudodata were then supplied back to the model as 'observations,' and posterior distributions for each parameter were estimated. A failure to obtain the same parameter values used to generate the data in the posterior distribution would indicate that the model is overparameterized and is incapable of accurately capturing the system dynamics.

Diel curves were generated over a 48-h period such that GPP was roughly equivalent to ER and both were greater than G. The depth of the model system was set to 30 cm with a hypothetical area of 1 m^2. Water temperature was held constant at 20°C. For error in precision tests, random deviations were applied to diel data following a normal distribution, with initial standard deviations of $\pm$ 0.1 mg L^{-1} and $\pm$ 0.2‰ for $[O_2]$ and $\delta^{18}O–O_2$, respectively. This level of error approximated observed variation from repeated measurements in the field using collection methods described below. Standard deviations were increased to 0.2 mg L^{-1}, 0.3‰ and 0.4 mg L^{-1}, 0.6‰ in two additional trials. Effects of errors in accuracy on ecosystem metabolism estimates were tested with the use of model-derived O_2 curves (no $\delta^{18}O–O_2$) given a constant bias in terms of percent saturation. The amount of bias ranged from 15% below the true value to 15% above the true value. The effect of data resolution on parameter estimates was tested by progressively increasing the interval between observations from 10 min to 4 h, with random errors of 0.1 mg L^{-1} and 0.2‰. Last, diel $[O_2]$ curves (no $\delta^{18}O–O_2$) of different magnitude were generated by varying GPP and the gas transfer velocity (k_{20}). GPP ranged from 0.62 to 7.4 g m^{-2} d^{-1}, whereas ER was held constant at 5.0 g m^{-2} d^{-1} (GPP:ER from 0.12 to 1.5). k_{20} ranged from 0.05 to 0.8 m h^{-1}. For scenarios that included $\delta^{18}O–O_2$ data, the isotopic ratio of oxygen in water ($\delta^{18}O–H_2O$) was held constant at the specified value of -5‰ because allowing this parameter to be estimated increases the posterior uncertainty, and in field situations, it is relatively easy and accurate to measure directly.

MCMC chains are from 1 to 5 million iterations and thinned to 1000 saved posterior draws. To test that MCMC chains had fully explored the posterior parameter space (convergence), the saved draws were tested for autocorrelation of $< 5\%$ for all parameters using the *acf* function in the CODA package of R (R Foundation) and by visual examination of parameter traces (Plummer et al. 2006).

Model applications to field data—We used BaMM to analyze one previously published diel oxygen data set and one new data set that reflect the metabolic properties of moderately productive lotic ecosystems. Previously published data were from the South Saskatchewan River (Saskatoon, Canada; Venkiteswaran et al. 2007). Available data included both $[O_2]$ and $\delta^{18}O–O_2$. Limited irradiance

data were also available, which was used to scale the irradiance submodel to local conditions.

We also estimated the metabolic properties of Pick Creek (59°33′4″N, 159°4′37″W), a third-order stream 7.5 m wide and ~ 2.5 km in length located within the Wood River system of southwest Alaska. Oxygen concentration and $\delta^{18}O$–O_2 samples were collected at a single station near the outflow hourly from 15:00 h 14 July 2008 to 20:00 h 15 July 2008, with breaks from 09:00–11:00 h and 21:00–23:00 h. Water temperature and $[O_2]$ were recorded at 10-min intervals with a YSI 6600 V2 sonde equipped with a optical dissolved oxygen (ROx) sensor. Sensor $[O_2]$ measurements were calibrated to $[O_2]$ measurements from dissolved gas ratios described below. Irradiance at the water surface was measured directly in 10-min intervals at a field station 2.4 km away with a LI-COR LI-192 quantum sensor (LI-COR Biosciences).

The $\delta^{18}O$–O_2 and $[O_2]$ in water samples were determined by methods similar to Barth et al. (2004) and are briefly explained here. Twelve-milliliter glass sample vials with butyl septa (Exetainers®, Labco) were washed with soap and water, ashed to 500°C, coated with a 40 μL of saturated mercuric chloride as a preservative, and flushed with He to remove all atmospheric O_2 2–6 weeks before sampling. In the field, samples were collected by fully immersing vials under water, opening each vial until completely filled with stream water, and capping vials underwater, being careful not to contaminate with atmospheric air. After returning from the field each day, vials were injected with an additional 50 μL of mercuric chloride through the septa to ensure that all biological activity has ceased. Septa were coated with a small amount of silicone grease to avoid air leaks. Samples were analyzed within 2 months at the University of Washington (UW) Oceanography Stable Isotope Lab. One day before analysis, pure helium was pumped into the vial until roughly half the water was displaced. Isotopic ratios of headspace gases were determined by simultaneously measuring masses 32, 34, and 40 (^{18}O–^{16}O, ^{16}O–^{16}O, and ^{40}Ar) on a Finnigan Delta XL continuous-flow mass spectrometer (Thermo Electron). Dissolved oxygen concentrations were calculated based on the O_2 : Ar (masses 32 and 40) and the dissolved Ar concentration as a function of water temperature (Weiss 1970; Emerson et al. 1999). A 30-mL sample of stream water from each sampling date was sent to the UW IsoLab for ^{18}O–H_2O isotope analysis. Isotopic ratios are expressed in δ notation and referenced to standard mean ocean water (SMOW) according to the following equation with units of per mil (‰):

$$\delta^{18}O = \frac{\frac{18}{16}O_{sample}}{\frac{18}{16}O_{SMOW}} \times 1000 \qquad (12)$$

Analytical error based on 62 duplicate samples was $\pm$ 0.1 mg L^{-1} and $\pm$ 0.2‰ ($\pm$ 1 SD) for $[O_2]$ and $\delta^{18}O$–O_2, respectively.

Field data were analyzed with uniform priors on all parameters, encompassing a broad range of plausible values, except for $\delta^{18}O$–H_2O and α_R (Pick Creek). The α_R for Pick Creek was fixed at the upper boundary of 1.000

because initial trials indicated values less than 1.000 were highly unlikely given the data, and allowing this parameter to be free interfered with the estimation of the remaining parameters. We used field data to test for parameter estimates that differed when using $[O_2]$ only vs. both $[O_2]$ and $\delta^{18}O$–O_2 budgets. When testing both $[O_2]$ and $\delta^{18}O$–O_2, concentration data were thinned to match isotope measurements so that each contributed equally to parameter estimates. When testing $[O_2]$ only, we performed trials using all available data at the highest temporal resolution possible (i.e., sonde data at 10- or 15-min intervals) and at approximately hour resolution. MCMC chains and convergence tests were the same as those for model validate scenarios.

Model implementation—BaMM was developed with the use of Automatic Differentiation Model Builder (ADMB; http://admb-project.org), an open-source software package specifically designed for function minimization and nonlinear statistical modeling. The oxygen and light submodels are compiled with existing ADMB routines for differentiation and MCMC estimation into a stand-alone executable program. We have also developed a Microsoft Excel® application that interfaces with BaMM to simplify data entry and control of modeling scenarios. The applications and a user manual are available via the GreenBoxes code-sharing network (http://conserver.iugo-cafe.org/user/gholtgrieve/BaMM).

Results

Model scenarios—BaMM successfully recaptured all parameters across a wide range of precision error in $[O_2]$ and $\delta^{18}O$–O_2 measurements (Table 3)—known model input parameters and rates of ecosystem metabolism were within the posterior distributions produced by BaMM. In addition, the standard errors of the observations (σ) were accurately estimated as free parameters. The 95% credible intervals (CI) of the posterior distributions were larger with a greater degree of error applied to the data. In general, estimates of α_{P-I} were most affected by precision errors with up to 30% deviation from the 'true' value for the 97.5% credible limit (CL) at the highest level of error. The remaining parameters appeared to be equally robust with respect to observation error, with maximum deviations of approximately 12% (97.5% CL). Estimates of metabolic rates were also highly constrained, even with significant precision error; 97.5% CL estimates of GPP, ER, and G were 12%, 13%, and 16%, respectively, of the true value. The mean values of posterior distributions for parameter and metabolism estimates were also affected by precision error. At the lowest level of error, posterior means were within 2% of the simulated true values. At higher levels of error, mean values were generally within 5% of the true values.

Data resolution tests showed that BaMM accurately recovered parameters at intervals commonly employed in field studies (Table 4). All initial parameter values were recovered in the posterior distributions, and, as the interval between data points increased, the precision and accuracy

Table 3. Results of model validation scenarios—precision error.

Random normal error SD ([O_2], $\delta^{18}O$–O_2)	Original input value	BaMM estimates		
		0.1,0.2	0.2,0.3	0.4,0.6
P_{max} (mg O_2 m^{-2} h^{-1})	400	405(390,417)	414(390,438)	408(369,450)
$\alpha_{P\text{-}I}$ (mg O_2 s μE^{-1} h^{-1})	1.8	1.8(1.6,2.0)	2.1(1.7,2.5)	1.7(1.3,2.3)
R_{20} (mg O_2 m^{-2} h^{-1})	310	310(300,320)	323(303,344)	312(281,347)
k_{20} (m h^{-1})	0.15	0.15(0.15,0.16)	0.15(0.15,0.17)	0.15(0.13,0.17)
α_R	0.990	0.990(0.990,0.990)	0.990(0.990,0.991)	0.990(0.988,0.992)
Initial [O_2] (mg L^{-1})	11.4	11.3(11.2,11.5)	11.6(11.3,12.0)	11.7(11.2,12.3)
Initial $\delta^{18}O$–O_2 (‰ vs. SMOW)	19.4	19.4(19.1,19.7)	19.6(19.1,20.2)	19.9(18.8,20.9)
GPP (g O_2 m^{-2} d^{-1})	5.2	5.3(5.1,5.4)	5.4(5.1,5.8)	5.3(4.8,5.8)
ER (g O_2 m^{-2} d^{-1})	5.2	5.2(5.1,5.4)	5.4(5.0,5.7)	5.2(4.8,5.8)
G (g O_2 m^{-2} d^{-1})	3.4	3.4(3.4,3.6)	3.5(3.2,3.8)	3.4(3.0,3.9)
[O_2] error (σ)		0.10(0.08,0.12)	0.23(0.19,0.29)	0.34(0.28,0.42)
$\delta^{18}O$–O_2 error (σ)		0.19(0.16,0.24)	0.31(0.25,0.38)	0.67(0.55,0.83)

GPP, gross primary production; ER, ecosystem respiration; G, total mass flux via gas exchange; SMOW, standard mean ocean water.
Parameter estimates from BaMM are given as mean (2.5% CL, 97.5% CL); CL, credible limits of posterior distribution.

of posterior results suffered. $\alpha_{P\text{-}I}$ was again the parameter most sensitive to data resolution, with $> 80\%$ deviation from the true value (97.5% CL) when data were at 4-h intervals. There was relatively little change in posterior results going from 10-min to 0.5-h data intervals; posterior credible intervals increased with each step from 1- and 4-h data resolution. At data intervals of ≥ 6 h, the model failed to converge on unique solutions.

Errors in the accuracy of dissolved oxygen measurements had a significant effect on metabolism estimates (Fig. 2). The regression slope between the amount of bias added to the diel O_2 data and the resultant mean posterior ecosystem metabolism estimate was 1.1 ± 0.05 for GPP and -5.0 ± 0.03 for ER. Therefore, errors in GPP estimates roughly scale with the amount of bias in the dissolved oxygen measurements (i.e., a 1% error in accuracy of dissolved oxygen measurements translates to a 1% deviation in GPP), whereas ER is about five times more sensitive to accuracy errors. Gas transfer velocity (k_{20}) estimates are unaffected by shifts in the diel curve up or down (slope = 0.1 ± 0.1) because this parameter is mostly determined by the transient responses of O_2 to changing irradiance.

Using model scenarios, we compared the effects of increasing k_{20} with different levels of GPP (Fig. 3). We found the model accurately recovered input parameters when diel dissolved oxygen changes were greater than ~ 1.5 mg L^{-1} and 2–4‰. As the diel signal diminished relative to the amount of precision error, both the accuracy and precision of the posterior distributions declined. Increasing k_{20} increased the 95% CL across all levels of GPP (Fig. 3c–f). At the highest level of k_{20} (0.8 m h^{-1}), estimated GPP deviated from the true GPP by 17% (maximum of 81% at the 97.5% CL), compared with $< 1\%$ (maximum $< 5\%$) when k_{20} was only 0.05 m h^{-1}. Higher k_{20} does not always translate into greater O_2 mass flux across the air–water interface because mass flux depends on both the gas transfer velocity and O_2 concentration gradient (Venkiteswaran et al. 2008). The primary effect of increased k_{20} is diminished daytime dissolved oxygen peaks and a more rapid onset and longer duration of the nighttime dissolved oxygen plateau

(Fig. 3a,b). As the diel curve flattens, the ability of the model to estimate metabolic parameters declines (although it remains remarkably good for reasonable k_{20} values, i.e., < 0.4 m h^{-1}). Increasing GPP partially offsets the effect of increasing k_{20}, such that the smallest average and maximum deviations from the true GPP were generally at high GPP and vice versa (Fig. 3c–f).

Analysis of field data—We used Akaike's Information Criterion corrected for small sample size (AICc; Burnham and Anderson 2002) to compare the model fit with data, assuming either the linear or light-saturating production function (Fig. 4). Analysis of the South Saskatchewan River data showed substantially more support for the light-saturating model (Eq. 1), with a difference in AICc (ΔAICc) of 47.8 compared with the linear model (ΔAICc values > 10 indicates the model with the lower AICc has considerably more empirical support, whereas values < 2 indicate roughly equivalent models; Burnham and Anderson 2002).

The saturating model did a better job of predicting dissolved oxygen pools (Fig. 4), particularly at the midday light and [O_2] maximum, which constrained the posterior distributions of GPP, ER, and G (Fig. 5f–h). Posterior estimates of daily integrated ecosystem metabolic rates for the South Saskatchewan River under a light-saturating production model were 11.5 ± 0.3 g m^{-2} d^{-1} for GPP, 10.4 ± 0.2 g m^{-2} d^{-1} for ER, and 5.3 ± 0.2 g m^{-2} d^{-1} for G (mean ± 1 SD; Fig. 5f–h). These rates were significantly larger than estimates assuming a linear model (9.6 ± 0.4, 9.1 ± 0.4, and 4.7 ± 0.5 g m^{-2} d^{-1}, respectively) because of the relatively high O_2 production at lower light levels. The mean posterior values of $\alpha_{P\text{-}I}$ and R_{20} were higher when assuming light saturation. The posterior distribution of $\alpha_{P\text{-}I}$ also had a substantially larger credible interval (Fig. 5b, c). Estimates of the gas transfer velocity (k_{20}) for the South Saskatchewan River were both highly constrained and relatively unaffected by the different production models (Fig. 5d). Posterior 95% CIs of k_{20} were 0.072–0.105 m h^{-1} for the linear production model and 0.092–0.108 m h^{-1} for the light-saturating production model—somewhat lower

Table 4. Results of model validation scenarios—data resolution.

Data resolution	Original input value	BaMM estimates					
		10 min*	10 min and 1 h†	0.5 h†	1 h†	2 h†	4 h†
P_{max} (mg O₂ m⁻² h⁻¹)	400	401(393,408)	400(394,407)	399(390,408)	405(390,417)	402(385,418)	395(364,429)
α_{P-I} (mg O₂ s μE⁻¹ h⁻¹)	1.8	1.7(1.6,1.9)	1.7(1.6,1.8)	1.8(1.6,1.9)	1.8(1.6,2.0)	1.8(1.6,2.0)	1.8(1.1,3.3)
R_{20} (mg O₂ m⁻² h⁻¹)	310	308(302,313)	308(303,313)	304(296,311)	310(300,320)	308(294,321)	300(272,333)
k_{20} (m h⁻¹)	0.15	0.15(0.15,0.15)	0.15(0.15,0.15)	0.15(0.15,0.15)	0.15(0.15,0.16)	0.15(0.14,0.16)	0.14(0.13,0.16)
α_R	0.990		0.990(0.990,0.991)	0.990(0.989,0.990)	0.990(0.990,0.990)	0.990(0.989,0.990)	0.990(0.988,0.991)
Initial [O₂] (mg L⁻¹)	11.4	11.4(11.4,11.5)	11.4(11.4,11.5)	11.3(11.2,11.4)	11.3(11.2,11.5)	11.3(11.2,11.5)	11.4(11.1,11.7)
Initial δ18O–O₂ (‰ vs. SMOW)	19.4		19.4(19.1,19.8)	19.5(19.3,19.8)	19.4(19.1,19.7)	19.7(19.4,20.1)	19.6(18.9,20.1)
GPP (g O₂ m⁻² d⁻¹)	5.2	5.2(5.1,5.3)	5.2(5.1,5.3)	5.2(5.1,5.3)	5.3(5.1,5.4)	5.2(5.0,5.4)	5.1(4.6,5.7)
ER (g O₂ m⁻² d⁻¹)	5.2	5.1(5.0,5.2)	5.1(5.0,5.2)	5.1(4.9,5.2)	5.2(5.1,5.4)	5.1(4.9,5.3)	5.0(4.5,5.5)
G (g O₂ m⁻² d⁻¹)	3.4	3.4(3.3,3.4)	3.4(3.3,3.4)	3.3(3.2,3.4)	3.4(3.4,3.6)	3.4(3.2,3.6)	3.3(2.9,3.7)
[O₂] error (σ)	0.10	0.10(0.09,0.11)	0.10(0.09,0.11)	0.10(0.09,0.12)	0.10(0.08,0.12)	0.10(0.07,0.13)	0.15(0.10,0.24)
δ18O–O₂ error (σ)	0.20		0.19(0.16,0.23)	0.20(0.18,0.24)	0.19(0.16,0.24)	0.18(0.13,0.25)	0.28(0.18,0.46)

Model-derived diel data were given random normal error with SD = 0.1 mg L⁻¹ and 0.2‰.
GPP, gross primary production; ER, ecosystem respiration; G, total mass flux via gas exchange; SMOW, standard mean ocean water.
Parameter estimates from BaMM are given as mean (2.5% CL, 97.5% CL); CL = credible limits of posterior distribution.
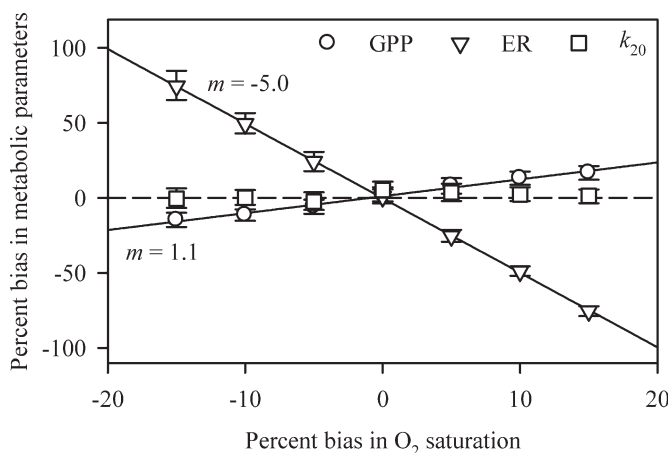* [O₂] only.
† [O₂] and δ18O–O₂.

Fig. 2. Effects of errors in accuracy of dissolved oxygen measurements on estimation of metabolic parameters. The original model-derived diel dissolved oxygen curve was generated with GPP ≈ ER (5 g m⁻² d⁻¹) and k_{20} = 0.15 m h⁻¹. Simulations did not include δ18O–O₂ data. Bias was added as a fixed percentage of percent saturation for each time step in the model (*x*-axis). [O₂] data were at hour intervals and given random normal error (± 0.1 mg L⁻¹). Data points are the difference in the mean estimated value vs. the known true value, expressed as a percentage of the known value (*y*-axis). Error bars are the 95% credible intervals. *m* is the slope of the least squares regressions between the biases in dissolved oxygen data and the resultant metabolism estimates (R^2 > 0.99, *p* > 0.001).

but still overlapping with the 0.107 m h⁻¹ estimated by Venkiteswaran et al. (2007).

Diel [O₂] and δ18O–O₂ swings in Pick Creek were small compared with South Saskatchewan River and other published data sets (Parker et al. 2005; Tobias et al. 2007; Venkiteswaran et al. 2007). The creek showed considerable metabolic activity, with supersaturated dissolved oxygen (> 110%) during the day and substantially undersaturated conditions at night, despite the countervailing effect of diel water temperature variation (Fig. 6b–d). Respiration was significant, with nighttime dissolved oxygen at 86% of saturation. The δ18O–O₂ never exceeded the atmospheric end member of 24.2‰, indicating that the system fractionation effect of respiration on dissolved oxygen was small (α_R ≈ 1; Fig. 6d).

BaMM was able to fit the observed data with a high degree of confidence (Fig. 6c,d). During the second daytime sampling, maximum light intensity was roughly half of the previous day because of cloud cover (Fig. 6a). Diel changes in dissolved oxygen pools were roughly the same between the two days however, suggesting a saturating response of O₂ production to irradiance. This was confirmed through model selection where the light saturation production function had significantly more support (ΔAICc = 174.3) and substantially better fits to the data.

With the use of [O₂] and δ18O–O₂ data from only the gas ratio collections, BaMM estimated GPP, ER, and G at 6.6 ± 0.3, 7.9 ± 0.3, and 4.4 ± 0.2 g m⁻² d⁻¹, respectively (mean ± 1 SD; Fig. 7e–g). The inclusion of oxygen isotopes provides a second, independent oxygen budget to constrain
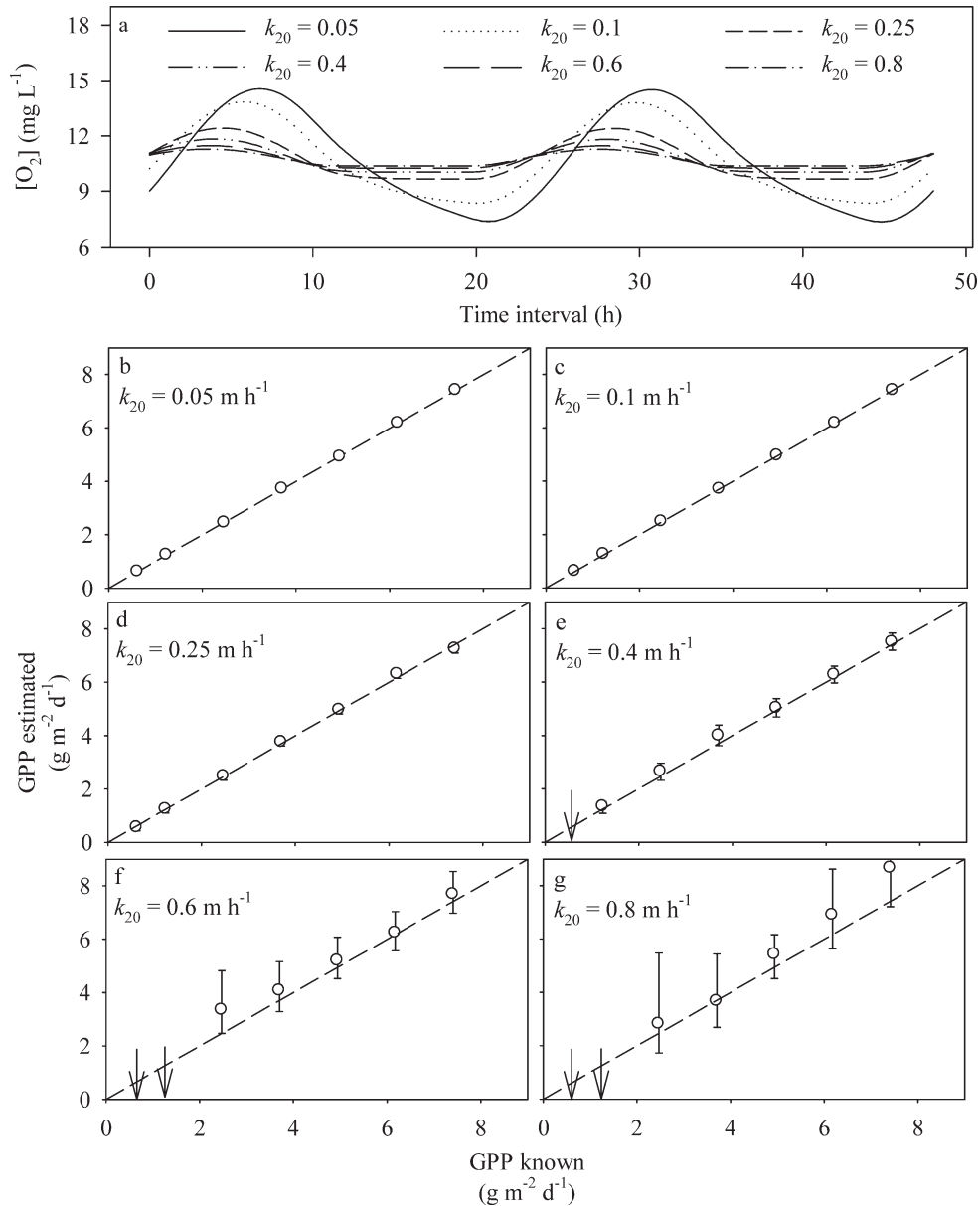
Fig. 3. Results of model tests to determine potential error in metabolic rate estimates with diminishing diel O_2 change. (a) The flattening of model-derived $[O_2]$ curve with increasing gas transfer velocity; oxygen trajectories shown are for GPP $\approx$ ER. Model scenarios were run across a range of metabolic states (GPP : ER ranging from 0.1 to 1.25) and gas transfer velocities. ER was held constant at 5 g O_2 m^{-2} d^{-1}. Data were at 10-min intervals and given random normal error (SD of $\pm$ 0.1 mg L^{-1}). (b–g) The estimated GPP posterior mean vs. the specified known GPP. Error bars are the 95% credible intervals. The dashed line is the 1 : 1 line. Arrows identify scenarios that failed to converge on unique solutions. A second analysis that also included the oxygen isotope budget showed nearly identical results (not shown).

the system. We expected that $\delta^{18}O$–O_2 data would provide critical information for constraining metabolism estimates by reducing cross-dependencies among parameters. However, tests from Pick Creek show that $[O_2]$ data was sufficient to estimate all the necessary parameters to generate metabolism estimates including k_{20} (Fig. 7). Parameter and ecosystem metabolism estimates obtained by high-resolution sonde $[O_2]$ data were somewhat lower

than estimates obtained with $[O_2]$ and $\delta^{18}O$–O_2 data from gas ratio collections, probably because of slight differences in $[O_2]$ between the two techniques. Mean posterior values of GPP, ER, and G were within 12%, 8%, and 7%, respectively, of each other. Posterior distributions were substantially more constrained with the use of higher resolution data, as opposed to including the second oxygen budget. Similar results were also obtained for the South
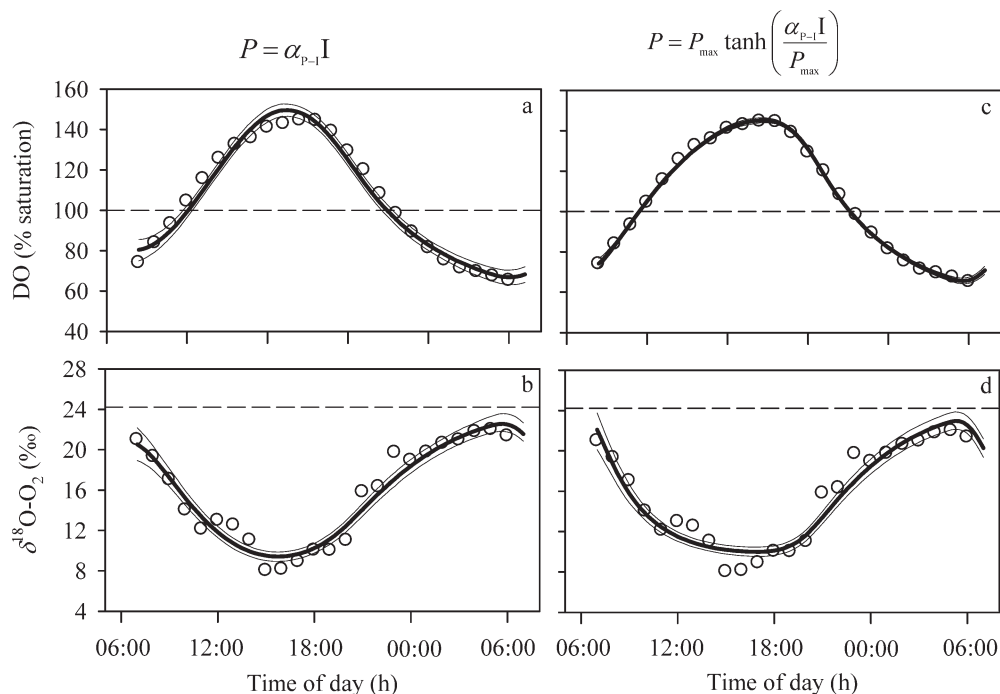
$$P = \alpha_{\mathrm{P-I}} \mathrm{I}$$

$$P = P_{\max} \tanh\left(\frac{\alpha_{\mathrm{P-I}} \mathrm{I}}{P_{\max}}\right)$$

Fig. 4. BaMM fits to diel dissolved oxygen (DO, expressed in percentage of saturation) and $\delta^{18}O$–O_2 data from the South Saskatchewan River with the use of either (a–b) a linear production function or (c–d) a light-saturating production model (*see* text for description of production models). Thick (center) lines are the median predicted DO and $\delta^{18}O$–O_2 from 1000 saved posterior MCMC draws, whereas the thin (outer) lines are the 2.5% and 97.5% credible limits. Horizontal dashed lines show conditions at equilibrium with the atmosphere. Fits to observed data were substantially better using the saturating production assumption based on differences in the Akaike's Information Criterion between the two models (ΔAICc = 47.8). Data are from Venkiteswaran et al. (2007).

Saskatchewan River, with mean posterior values essentially unchanged, and more constrained posterior distributions using high-resolution $[O_2]$ data (Fig. 8).

Gas transfer velocity (k_{20}) estimates for Pick Creek using uniform priors ranged from 0.25 to 0.30 m h^{-1} and were similar among data sets (Fig. 7d). Predicted values of k_{20} from three empirical relationships of stream slope, discharge, and water current velocity were 0.20, 0.37, and 0.78 m h^{-1} based on the models of O'Connor and Dobbins (1958), Melching and Flores (1999), and Tsivoglou and Neal (1976), respectively. We also performed tracer additions of sulfur hexafluoride (SF$_6$) and estimated k_{20} to be 0.13 m h^{-1} However, Pick Creek is a large stream with little mixing; as a result, the confidence limits from the regression analysis ranged from 0 to more than 0.81 m h^{-1} (essentially uninformative). Taken together, estimating k_{20} values on the basis of the likelihood of model predictions to observed data of oxygen dynamics produced a constrained estimate of the gas transfer velocity that was reasonable given known empirical relationships.

We calculated GPP and ER for Pick Creek using the standard difference method (Odum 1956; Bott 2006) as a comparison to BaMM-derived estimates (Table 5). GPP estimates from BaMM were from 2–21% higher than for the difference method when k_{20} was fixed as a constant; ER was within 4–8%. Differences between the two methods

likely arise from the subjectivity of specifying when nighttime starts and stops and the lack of temperature-dependent respiration when using the difference method. Methods for incorporating prior information on k_{20} greatly influenced results. k_{20} is directly specified without error when using the difference method, and higher values resulted in higher estimated rates of GPP and ER. This was the case when k_{20} was set as a constant in BaMM as well. k_{20} was also supplied to BaMM as a uniform range of equally probable values and as a normal distribution on the basis of SF$_6$ evasion measurements. In both cases, allowing k_{20} to be estimated based on these prior assumptions and model fits to the data resulted in estimated values of 0.27 $\pm$ 0.01 m h^{-1} and substantially higher rates of GPP and ER (Table 5).

In contrast to the South Saskatchewan River, which was an autotrophic system (GPP : ER = 1.1 $\pm$ 0.02 SD) with a low gas transfer velocity and high light intensity, Pick Creek was a heterotrophic system (GPP : ER = 0.83 $\pm$ 0.01 SD) with a relatively high gas transfer velocity (although a roughly equivalent mass flux, G) and relatively low light. The posterior results of modeled primary productivity showed that the two systems differ significantly in their P-I relationships (Fig. 9). Pick Creek had a significantly lower $P_{\max}$ and higher $\alpha_{\mathrm{P-I}}$ than the South Saskatchewan River, indicating the system to be more adapted to a low-light
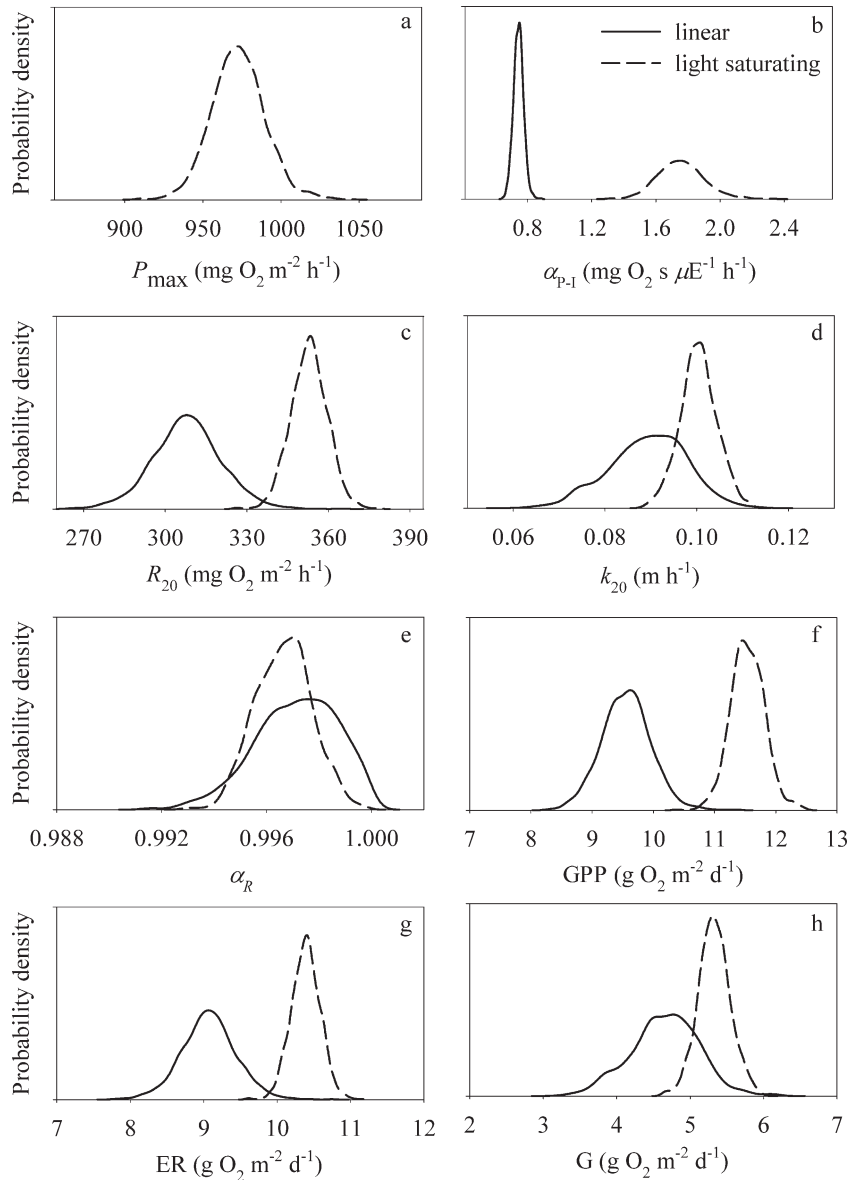
Fig. 5. Posterior probability distributions of model parameters and metabolic rates derived from Bayesian analysis of diel [O_2] and $\delta^{18}O$–O_2 data from the South Saskatchewan River (Venkiteswaran et al. 2007). Solid lines are results from a linear production model, whereas dashed lines are from a light-saturating model.

environment. These ecosystem-scale results are also consistent with physiological studies under controlled conditions that show there is an inherent trade-off between maximum photosynthetic capacity and production at low light levels (Fig. 9 inset; Guasch and Sabater 1995; Hill et al. 1995).

Discussion

A consistent challenge for ecological analysis is to extract the full information contained in data. Analysis within a modeling framework has only recently been applied to ecosystem metabolism research and incorporates important transient dynamics in determining metabolic

parameters (Van de Bogert et al. 2007; Venkiteswaran et al. 2007; Hanson et al. 2008). For example, the relative magnitude of dissolved oxygen change in response to diel irradiance cycles is the basis for estimating photosynthesis–irradiance parameters (P_{max} and α_{P-I}). Similarly, the degree to which dissolved oxygen changes lag behind irradiance and the presence of a nighttime plateau provides information about the gas transfer velocity (k); estimates of k_{20} are therefore most reliable when using measured irradiance data. Finally, the change in $\delta^{18}O$–O_2 relative to [O_2] provides information on in situ fractionation of dissolved oxygen with respiration.

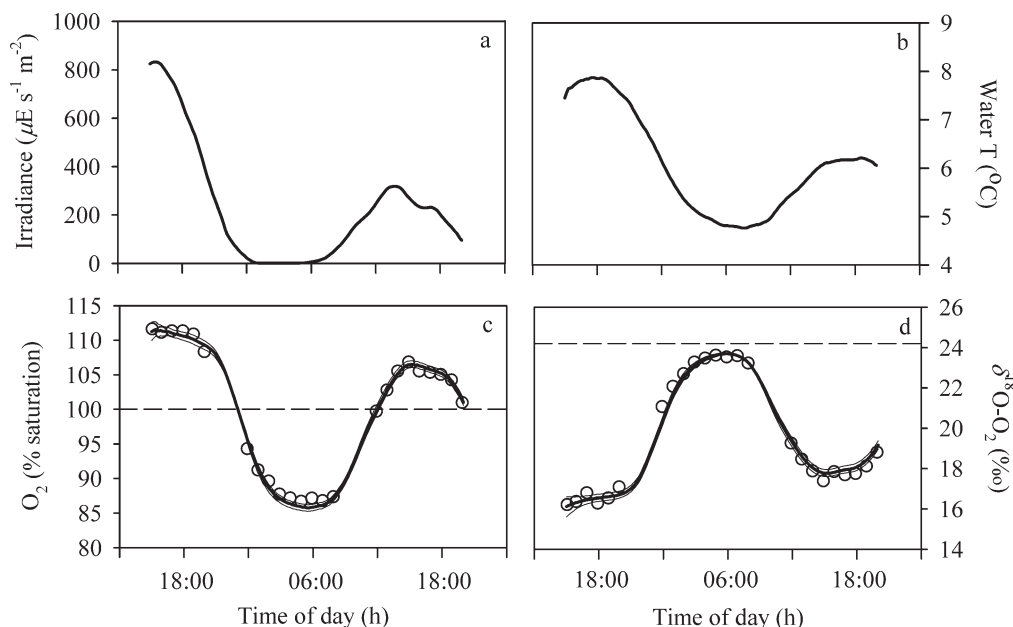Previous metabolism methods based on either diel dissolved oxygen cycles or steady state assumptions suffer

Fig. 6.   BaMM fits to dissolved oxygen (DO, expressed in percentage of saturation) and $\delta^{18}O$–O_2 data from Pick Creek, 14–15 July 2008. The model was fit using (a) measured irradiance and (b) water temperature with a light-saturating production model. (c, d) Thick (center) lines are the posterior median predicted DO and $\delta^{18}O$–O_2, whereas the thin (outer) lines are the 2.5% and 97.5% credible limits. Horizontal dashed lines show conditions at equilibrium with the atmosphere.

by requiring the deterministic specification of a gas transfer velocity—a difficult measurement to make—and by not fully exploiting high-resolution data over diel cycles to examine critical biological and physical relationships. Diel curves that show a gradual decline in O_2 pools at night and large O_2 increases during the day will provide the best estimates of ecosystem metabolism and k_{20}. These are low-k, high-productivity systems with metabolic rates that are a substantial fraction of dissolved oxygen pools. In contrast, high-k systems will come into rapid equilibrium, and dissolved oxygen will track irradiance and water temperature tightly, generating a prolonged nighttime plateau and reducing the amount of information in the data. The result is larger posterior credible intervals and higher uncertainty in ecosystem metabolism estimates. In evaluating model fits to the data, it is important to consider whether the model adequately reproduces the shape of the diel curves because many of the key parameters (k, in particular) modify the shape of the curve, as well as the magnitude of diel swings (Venkiteswaran et al. 2008). Ecosystems with ER substantially larger than GPP and roughly equivalent to G will approach a steady-state condition and not be constrained by BaMM (i.e., the model fails to converge). This is also true for systems in which daily metabolic rates are less than $\sim$ 10% of the total oxygen pool. In these situations, additional prior information on parameters such as k_{20} is necessary to constrain the system, and results will be highly dependent on these priors.

Tests from Pick Creek and the South Saskatchewan River show that ecosystem metabolism and reaeration can be accurately estimated in moderate- to high-productivity systems with the use of diel oxygen concentration data alone. BaMM metabolism estimates are comparable to

standard difference methods when specifying k_{20} as a constant that is assumed to be known without error. Allowing BaMM to estimate this parameter will give significantly different estimates of metabolism when the data are highly informative and the model estimated values differ substantially from prior information.

Field data tests also suggest that increased data resolution provides more information for parameter estimation than a second oxygen budget, both because of the amount of information contained in high-resolution data and the fewer number of estimated parameters in the model. The benefit of more data over a second oxygen budget is likely dependent on the dynamics of specific systems. The oxygen isotopic ratio of water ($\delta^{18}O$–H_2O) and system α_R will affect the daytime declines and nighttime peaks in the $\delta^{18}O$–O_2 curves and therefore the diel change in dissolved oxygen isotopes relative to [O_2]. In certain cases such as high–gas exchange, high-ER systems with distinct isotopic end members, including diel $\delta^{18}O$–O_2 curves might substantially improve results. More diel dual and triple oxygen isotope measurements across a variety of ecosystem types are necessary to fully understand when dissolved oxygen isotope budgets provide significant additional information. As of now, it appears these techniques are most useful in open systems with large, well-mixed dissolved oxygen pools that are reasonably approximated by steady-state assumptions (i.e., ocean and large river systems). However, at least one study from coastal Japan has shown significant diel change in offshore waters for both dual and triple oxygen isotopes (Sarma et al. 2005), suggesting broad steady-state assumptions should be reconsidered.

Although model scenarios show that BaMM is robust to significant error in the precision of dissolved oxygen
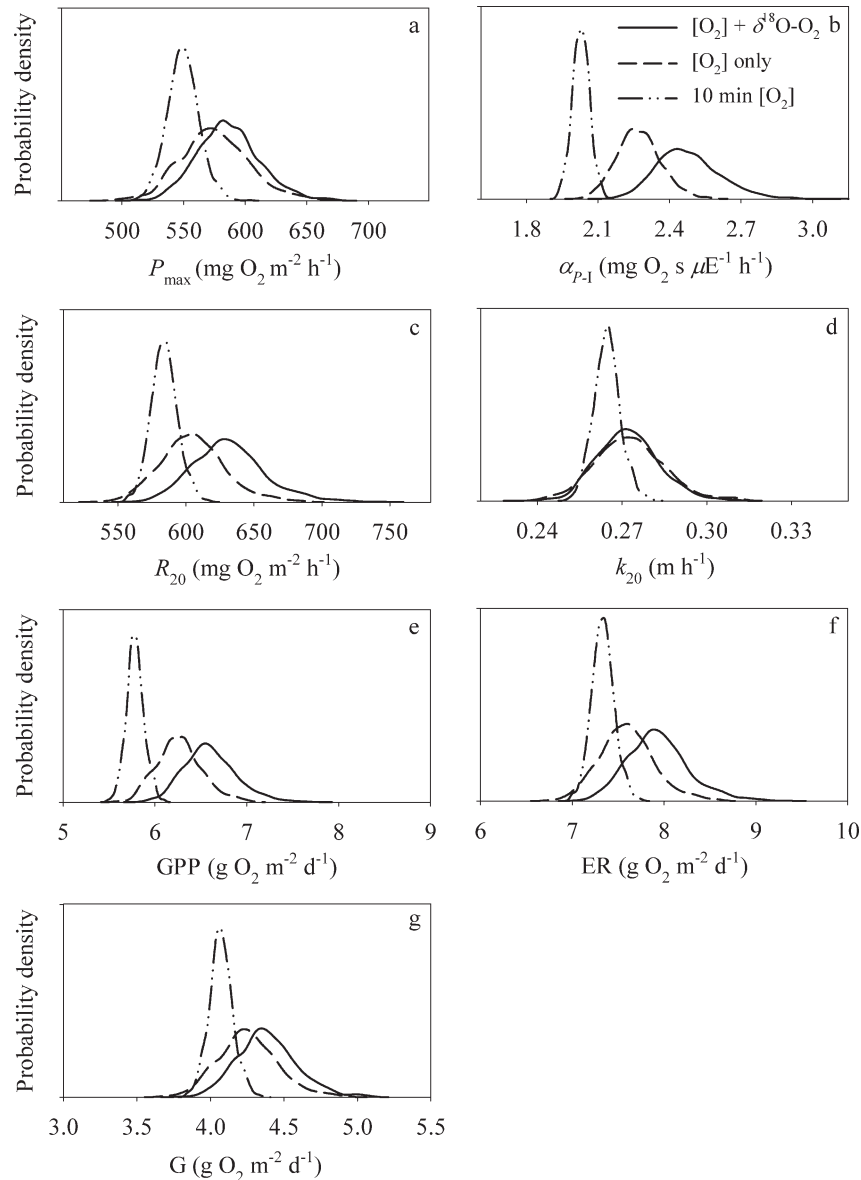
Fig. 7. Posterior probability distributions of model parameters and metabolic rates from Pick Creek diel oxygen data. Solid lines are posterior probability distributions of model parameters and metabolic rates when including both $[O_2]$ and $\delta^{18}O$–O_2 data from gas ratio collections. Dashed lines show results when including only the $[O_2]$ data. Dashed-dotted lines are results using $[O_2]$ data from an optical dissolved oxygen probe recorded at 10-min intervals and calibrated to the gas ratio measurements.

measurements (Table 3), this is likely an overly pessimistic test because this type of observation error is generally very low. Errors in accuracy of dissolved oxygen measurements on the other hand can substantially influence metabolism estimates, in particular ER, which affects the average daily O_2 saturation level (Fig. 2; Venkiteswaran et al. 2008). It is critical to ensure accuracy of dissolved oxygen measurements because this type of systematic error is not encapsulated in Bayesian posterior results. Errors are currently treated as random noise following a normal distribution. Parameter estimates can be skewed in systems with high variance and strongly autocorrelated errors;

however, this appears not to be a significant issue in the analysis of our field data.

If applied to lotic systems, the one-station method presented here assumes a stream channel without discontinuities (lakes, ponds, wetlands) or significant groundwater inputs. The distance upstream from a station that contributes to oxygen dynamics, in the absence of significant biological controls, can be estimated as $3vd/k$, where v is velocity (m h^{-1}), d is depth (m), and k is the gas transfer velocity (m h^{-1}; Chapra and DiToro 1991; M. Grace pers. comm.). Biological controls on oxygen will reduce this 'effective' distance in streams. The one-station
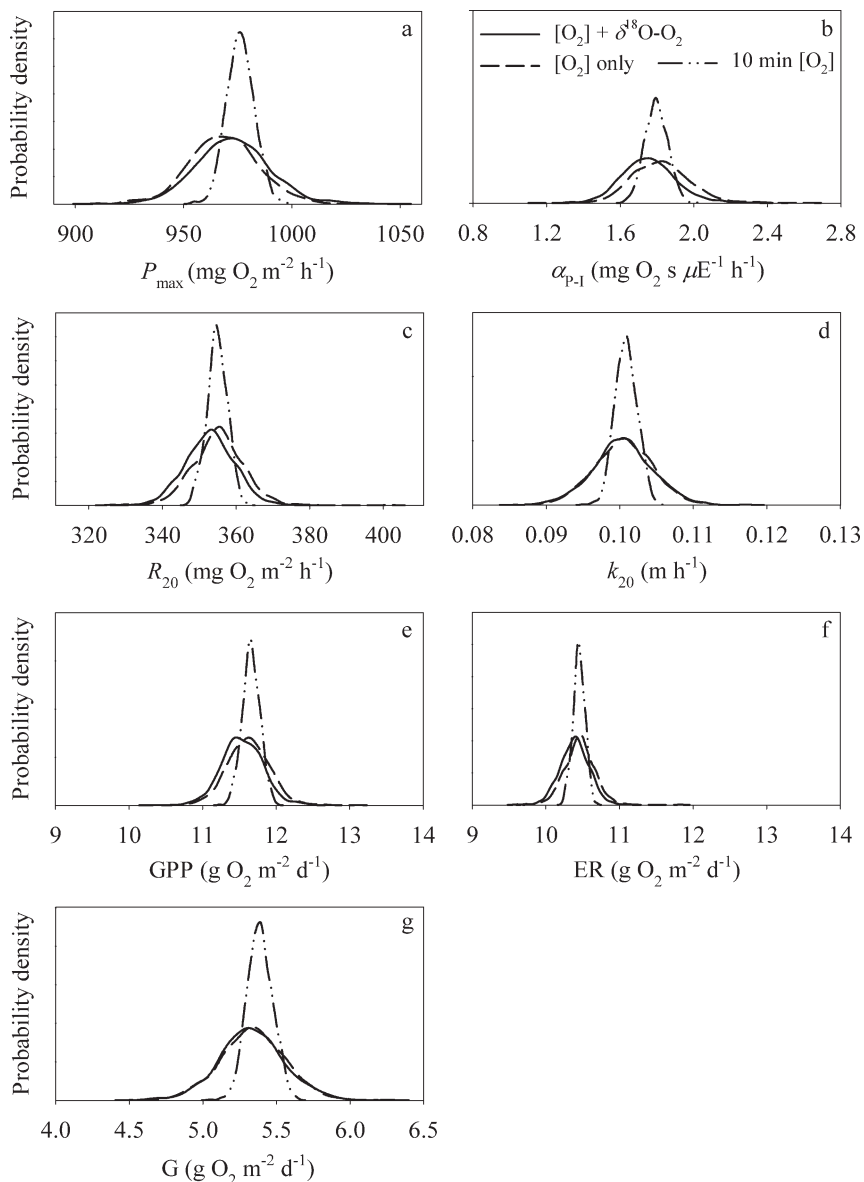
Fig. 8.   Results of Bayesian analysis of diel oxygen data from South Saskatchewan River. Solid lines are posterior probability distributions of model parameters and metabolic rates when including both $[O_2]$ and $\delta^{18}O$–O_2 data. Dashed lines show results when including only the $[O_2]$ data (hourly resolution). Dashed-dotted lines are results using $[O_2]$ data from a DO probe at 15-min intervals.

method assumes a well-mixed pool with little exchange between neighboring water masses with distinct oxygen dynamics. If trends in observed data do not fall within the best model fits, this suggests significant model error, and the assumptions associated with a one-station method of calculating ecosystem metabolism might be invalid.

The assumption that respiration is solely affected by temperature and not by other factors such as light is a common simplifying assumption necessary to constrain the model. ER estimates can therefore not be parsed into autotrophic vs. heterotrophic respiration with BaMM. If α_R is assumed to be known perfectly, it is possible to derive diel variation in ER with two oxygen budgets (and

therefore determine autotrophic respiration; Tobias et al. 2007). BaMM is currently not configured for such an analysis.

Testing for evidence of light-saturated production provides information into system dynamics and will potentially affect metabolism estimates. Ventikestwaran (2007) first analyzed the South Saskatchewan River data assuming no light saturation, with metabolism estimates significantly different from our estimates incorporating light saturation. Hanson et al. (2008) also used a similar model-fitting procedure for diel oxygen data from two lakes and found that increasing complexity of production models (including light saturation) did not improve the fit

Table 5. Comparison of ecosystem metabolism calculation methods.

k_{20}	Prior	Difference method GPP	ER	BaMM GPP	ER
0.20*	Constant	4.3	5.9	4.4(4.2,4.5)	5.7(5.5,5.8)
0.13†	Constant	2.9	4.1	3.5(3.2,3.7)	4.4(4.1,4.6)
0.13 ± 0.9†	Normal			5.3(5.2,5.5)	7.0(6.8,7.3)
0.27 ± 0.01‡	Uniform	5.6	7.9	5.8(5.6,6.0)	7.3(7.1,7.6)

Diel oxygen data (g O_2 m^{-2} d^{-1}) from Pick Creek 14–15 Jul 2008.
GPP, gross primary production; ER, ecosystem respiration; G, total mass flux via gas exchange.
Parameter estimates from BaMM given as mean (2.5% CL,97.5% CL).
* From O'Conner and Dobbins (1958) model of reaeration.
† From SF_6 tracer injection (± standard error of the regression).
‡ Estimated value from BaMM with a uniform prior. Applied to difference method as a constant.

Fig. 9. Photosynthesis–irradiance relationships for the South Saskatchewan River and Pick Creek under a light-saturating production model. Thick (center) lines are the mean predicted instantaneous *P* vs. irradiance. Thin (outer) lines are the 2.5% and 97.5% credible limits. Inset shows 1000 saved posterior MCMC draws of production model parameters (P_{max} vs. α_{P-I}).

to the data. Other studies have found evidence for light saturated production at the ecosystem scale (Young and Huryn 1999; Uehlinger et al. 2000), however, and how primary productivity scales from laboratory assays to whole ecosystems remains an unanswered question.

Bayesian analysis and prior information—Bayesian methods differ from simple optimization (e.g., sum of squares minimization or maximum likelihood) by considering both prior information and data to find high-likelihood regions for each parameter and integrate through these regions to generate probability distributions for model-predicted values. In contrast, optimization seeks to find the best fit to the data irrespective of how big the region of highly likely values might be. BaMM is constructed as an observation error–focused model and therefore assumes the underlying equations and relationships (e.g., relationship between light and photosynthesis, respiration and temperature) are deterministic. Observation error models generally tend to underestimate the full combination of observation, process, and model uncertainties (Polacheck et al. 1993), and as a result, posterior distributions represent the probabilities of model parameters under somewhat restrictive assumptions. State-space or hierarchical modeling frameworks have the potential to provide Bayesian posteriors that combine multiple types of error and are currently an active area of research (Cressie et al. 2009).

Prior information must be incorporated into the analysis through prespecified distributions. There is debate about the appropriateness of Bayesian methods in science, with those arguing against this approach citing inherent subjectivity in specifying priors and the strong influence that priors can have on posterior results (Lele and Dennis 2009). We believe that studies of biogeochemical processes are well suited for Bayesian analysis. It is often possible to measure or model key parameters (e.g., k_{20}), and these methods can have substantial yet quantifiable error, thereby removing much of the subjectivity of priors. Bayesian analysis is a robust methodology to use the full suite of available data in reducing that uncertainty. With
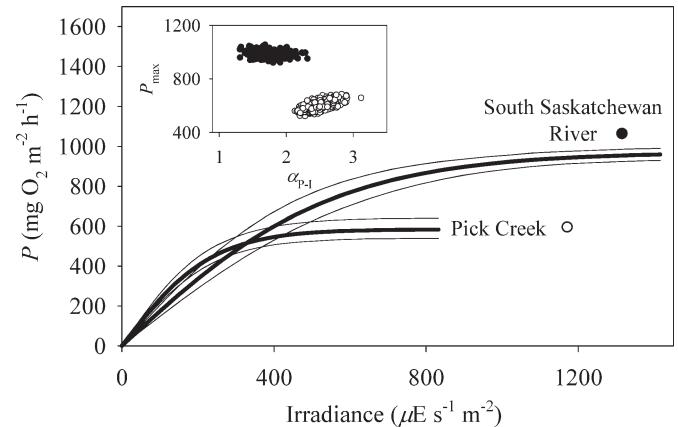
that said, we advocate caution in using prior information, such that the underlying assumptions are clearly specified and transparent so that others can judge whether the particular choices result in undue bias. We believe that using prior distributions determined experimentally combined with Bayesian methods can greatly reduce overall subjectivity in analysis and interpretation of biogeochemical data.

Advancements on previous methods—BaMM improves on traditional methods of ecosystem metabolism analysis in three important ways. First, reaeration can be determined directly from dissolved oxygen and irradiance data across a wide range of gas transfer velocities and metabolic conditions. Large, low-*k* systems are particularly suited for this analysis, and it is these systems in which ecosystem-scale measurements have so far proven difficult because of inadequate methods to determine *k*. Model estimates of k_{20} are best using measured irradiance because this parameter is sensitive to time lags between light and O_2 production, and model-derived irradiance might differ from field conditions. Second, by coupling irradiance data to O_2 dynamics using a model-fitting procedure, it is possible to derive fundamental relationships between light and primary productivity at the ecosystem scale. Furthermore, BaMM directly accounts for effects of changing water temperature on rates of gas exchange and respiration. The physical drivers of metabolism (temperature, irradiance) vary both spatially and temporally and these standardized metrics of ecosystem function allow for cross-system comparisons. Third, our model is intended to build on existing methodologies for ecosystem metabolism, and analysis of biogeochemical data in general, by providing methods to incorporate prior information and quantify error in the analysis. Including error estimates is essential when attempting to scale up station- or reach-scale measurements to larger spatial units. We encourage robust error analysis as a routine part of aquatic ecosystem

metabolism research. This approach will facilitate more systematic assessment of ecosystem metabolic parameters among sites and investigators, thereby enabling more rigorous synthesis of local- and global-scale productivity estimates of aquatic ecosystems.

References

BARTH, J. A. C., A. TAIT, AND M. BOLSHAW. 2004. Automated analyses of O-18/O-16 ratios in dissolved oxygen from 12-mL water samples. Limnol. Oceanogr. Methods **2:** 35–41.

BENSON, B. B., AND D. KRAUSE. 1984. The concentration and isotopic fractionation of oxygen dissolved in freshwater and seawater in equilibrium with the atmosphere. Limnol. Oceanogr. **29:** 620–632.

———, ———, AND M. A. PETERSON. 1979. Solubility and isotopic fractionation of gases in dilute aqueous solution. I. Oxygen. J. Solut. Chem. **8:** 655–690, doi:10.1007/BF01033696

BOTT, T. L. 2006. Primary productivity and community respiration, p. 663–690. *In* F. R. Hauer and G. A. Lamberti [eds.], Methods in stream ecology. Elsevier.

BURNHAM, K. P., AND D. R. ANDERSON. 2002. Model selection and multimodel inference: A practical information-theoretic approach, 2nd ed. Springer-Verlag.

CHAPRA, S. C., AND D. M. DITORO. 1991. Delta method for estimating primary production, respiration, and reaeration in streams. J. Environ. Eng. ASCE **117:** 640–655, doi:10.1061/(ASCE)0733-9372(1991)117:5(640)

CRESSIE, N., C. A. CALDER, J. S. CLARK, J. M. V. HOEF, AND C. K. WIKLE. 2009. Accounting for uncertainty in ecological analysis: The strengths and limitations of hierarchical statistical modeling. Ecol. Appl. **19:** 553–570, doi:10.1890/07-0744.1

EMERSON, S., P. D. QUAY, C. STUMP, D. WILBUR, AND R. SCHUDLICH. 1995. Chemical tracers of productivity and respiration in the subtropical Pacific Ocean. J. Geophys. Res. Oceans **100:** 15,873–15,887.

———, C. STUMP, D. WILBUR, AND P. QUAY. 1999. Accurate measurement of O_2, N_2, and Ar gases in water and the solubility of N_2. Mar. Chem. **64:** 337–347, doi:10.1016/S0304-4203(98)00090-5

FRANCIS, R., AND R. SHOTTON. 1997. "Risk" in fisheries management: A review. Can. J. Fish. Aquat. Sci. **54:** 1699–1715, doi:10.1139/cjfas-54-8-1699

GATES, D. M. 1966. Spectral distribution of solar radiation at the Earth's surface. Science **151:** 523–529, doi:10.1126/science.151.3710.523

GUASCH, H., AND S. SABATER. 1995. Seasonal variations in photosynthesis–irradiance responses by biofilms in Mediterranean streams. J. Phycol. **31:** 727–735, doi:10.1111/j.0022-3646.1995.00727.x

GUY, R. D., M. L. FOGEL, AND J. A. BERRY. 1993. Photosynthetic fractionation of the stable isotopes of oxygen and carbon. Plant Physiol. **101:** 37–47.

HANSON, P. C., S. R. CARPENTER, N. KIMURA, C. WU, S. P. CORNELIUS, AND T. K. KRATZ. 2008. Evaluation of metabolism models for free-water dissolved oxygen methods in lakes. Limnol. Oceanogr. Methods **6:** 454–465.

HELMAN, Y., E. BARKAN, D. EISENSTADT, B. LUZ, AND A. KAPLAN. 2005. Fractionation of the three stable oxygen isotopes by oxygen-producing and oxygen-consuming reactions in photosynthetic organisms. Plant Physiol. **138:** 2292–2298, doi:10.1104/pp.105.063768

HILBORN, R., AND M. MANGEL. 1997. The ecological detective: Confronting models with data. Princeton Univ. Press.

———, AND C. J. WALTERS. 1992. Quantitative fisheries stock assessment: Choice, dynamics and uncertainty. Chapman and Hall.

HILL, W. R., M. G. RYON, AND E. M. SCHILLING. 1995. Light limitation in a stream ecosystem: Responses by primary producers and consumers. Ecology **76:** 1297–1309, doi:10.2307/1940936

HOWARTH, R. W., AND A. F. MICHAELS. 2000. The measurement of primary production in aquatic ecosystems, p. 72–83. *In* O. E. Sala, R. B. Jackson, H. A. Mooney and R. W. Howarth [eds.], Methods in ecosystem science. Springer.

JASSBY, A. D., AND T. PLATT. 1976. Mathematical formulation of the relationship between photosynthesis and light for phytoplankton. Limnol. Oceanogr. **21:** 540–547.

JELLISON, R., AND J. M. MELACK. 1993. Meromixis in hypersaline Mono Lake, California. 1. Stratification and vertical mixing during the onset, persistence, and breakdown of meromixis. Limnol. Oceanogr. **38:** 1008–1019.

JURANEK, L. W., AND P. D. QUAY. 2005. In vitro and in situ gross primary and net community production in the North Pacific Subtropical Gyre using labeled and natural abundance isotopes of dissolved O_2. Glob. Biogeochem. Cycle **19:** GB3009, doi:10.1029/2004gb002384

KNOX, M., P. D. QUAY, AND D. WILBUR. 1992. Kinetic isotope fractionation during air–water gas transfer of O_2, N_2, CH_4 and H_2. J. Geophys. Res. Oceans **97:** 20,335–20,343.

KROOPNICK, P. M. 1975. Respiration, photosynthesis, and oxygen isotope fractionation in oceanic surface water. Limnol. Oceanogr. **20:** 981–988.

———, AND H. CRAIG. 1972. Atmospheric oxygen-isotopic composition and solubility fraction. Science **175:** 54–55, doi:10.1126/science.175.4017.54

LELE, S. R., AND B. DENNIS. 2009. Bayesian methods for hierarchical models: Are ecologists making a Faustian bargain. Ecol. Appl. **19:** 581–584, doi:10.1890/08-0549.1

LINDEMAN, R. L. 1942. The trophic–dynamic aspect of ecology. Ecology **23:** 399–417, doi:10.2307/1930126

LUZ, B., AND E. BARKAN. 2000. Assessment of oceanic productivity with the triple-isotope composition of dissolved oxygen. Science **288:** 2028–2031, doi:10.1126/science.288.5473.2028

MARZOLF, E. R., P. J. MULHOLLAND, AND A. D. STEINMAN. 1994. Improvements to the diurnal upstream–downstream dissolved oxygen change technique for determining whole-stream metabolism in small streams. Can. J. Fish. Aquat. Sci. **51:** 1591–1599, doi:10.1139/f94-158

McCree, K. J. 1972. Test of current definitions of photosynthetically active radiation against leaf photosynthesis data. Agric. Meteorol. **10:** 443–450, doi:10.1016/0002-1571(72)90045-3

Melching, C. S., and H. E. Flores. 1999. Reaeration equations derived from US geological survey database. J. Environ. Eng. ASCE **125:** 407–414, doi:10.1061/(ASCE)0733-9372(1999)125:5(407)

Mulholland, P. J., J. N. Houser, and K. O. Maloney. 2005. Stream diurnal dissolved oxygen profiles as indicators of in-stream metabolism and disturbance effects: Fort Benning as a case study. Ecol. Indic. **5:** 243–252, doi:10.1016/j.ecolind.2005.03.004

O'Connor, D. J., and W. E. Dobbins. 1958. Mechanism of reaeration in natural streams. Trans. Am. Soc. Civ. Eng. **123:** 641–684.

Odum, H. T. 1956. Primary production in flowing waters. Limnol. Oceanogr. **1:** 102–117.

Parker, S. R., S. R. Poulson, C. H. Gammons, and M. D. Degrandpre. 2005. Biogeochemical controls on diel cycling of stable isotopes of dissolved O_2 and dissolved inorganic carbon in the Big Hole River, Montana. Environ. Sci. Technol. **39:** 7134–7140, doi:10.1021/es0505595

Plummer, M., N. Best, K. Cowles, and K. Vines. 2006. CODA: Convergence diagnosis and output analysis for MCMC. R News **6:** 7–11.

Polacheck, T., R. Hilborn, and A. E. Punt. 1993. Fitting surplus production models—comparing methods and uncertainty. Can. J. Fish. Aquat. Sci. **50:** 2597–2607, doi:10.1139/f93-284

Quay, P. D., D. O. Wilbur, J. E. Richey, A. H. Devol, R. Benner, and B. R. Forsberg. 1995. The O-18/O-16 of dissolved-oxygen in rivers and lakes in the Amazon basin: Determining the ratio of respiration to photosynthesis rates in freshwaters. Limnol. Oceanogr. **40:** 718–729.

Quinones-Rivera, Z. J., B. Wissel, D. Justic, and B. Fry. 2007. Partitioning oxygen sources and sinks in a stratified, eutrophic coastal ecosystem using stable oxygen isotopes. Mar. Ecol. Prog. Ser. **342:** 69–83, doi:10.3354/meps342069

Roberts, B. J., P. J. Mulholland, and W. R. Hill. 2007. Multiple scales of temporal variability in ecosystem metabolism rates: Results from 2 years of continuous monitoring in a forested headwater stream. Ecosystems **10:** 588–606, doi:10.1007/s10021-007-9059-2

Sarma, V., O. Abe, S. Hashimoto, A. Hinuma, and T. Saino. 2005. Seasonal variations in triple oxygen isotopes and gross oxygen production in the Sagami Bay, central Japan. Limnol. Oceanogr. **50:** 544–552.

Stevens, C. L. R., D. Schultz, C. Vanbaalen, and P. L. Parker. 1975. Oxygen isotope fractionation during photosynthesis in a blue-green and a green alga. Plant Physiol. **56:** 126–129, doi:10.1104/pp.56.1.126

Tobias, C. R., J. K. Bohlke, and J. W. Harvey. 2007. The oxygen-18 isotope approach for measuring aquatic metabolism in high-productivity waters. Limnol. Oceanogr. **52:** 1439–1453.

———, ———, ———, and E. Busenberg. 2009. A simple technique for continuous measurement of time-variable gas transfer in surface waters. Limnol. Oceanogr. Methods **7:** 185–195.

Tsivoglou, E. C., and L. A. Neal. 1976. Tracer measurement of reaeration: Predicting reaeration capacity of inland streams. J. Water Pollut. Control Fed. **48:** 2669–2689.

Uehlinger, U., C. Konig, and P. Reichert. 2000. Variability of photosynthesis–irradiance curves and ecosystem respiration in a small river. Freshw. Biol. **44:** 493–507, doi:10.1046/j.1365-2427.2000.00602.x

Van de Bogert, M. C., S. R. Carpenter, J. J. Cole, and M. L. Pace. 2007. Assessing pelagic and benthic metabolism using free water measurements. Limnol. Oceanogr. Methods **5:** 145–155.

Venkiteswaran, J. J., S. L. Schiff, and L. I. Wassenaar. 2008. Aquatic metabolism and ecosystem health assessment using dissolved O-2 stable isotope diel curves. Ecol. Appl. **18:** 965–982, doi:10.1890/07-0491.1

———, L. I. Wassenaar, and S. L. Schiff. 2007. Dynamics of dissolved oxygen isotopic ratios: A transient model to quantify primary production, community respiration, and air–water exchange in aquatic ecosystems. Oecologia **153:** 385–398, doi:10.1007/s00442-007-0744-9

Wanninkhof, R. 1992. Relationship between wind-speed and gas exchange over the ocean. J. Geophys. Res. Oceans **97:** 7373–7382, doi:10.1029/92JC00188

Weiss, R. F. 1970. Solubility of nitrogen, oxygen and argon in water and seawater. Deep-Sea Res **17:** 721–735.

Yacobi, Y. Z., N. Perel, E. Barkan, and B. Luz. 2007. Unexpected underestimation of primary productivity by O-18 and C-14 methods in a lake: Implications for slow diffusion of isotope tracers in and out of cells. Limnol. Oceanogr. **52:** 329–337.

Young, R. G., and A. D. Huryn. 1999. Effects of land use on stream metabolism and organic matter turnover. Ecol. Appl. **9:** 1359–1376, doi:10.1890/1051-0761(1999)009[1359:EOLUOS]2.0.CO;2